Am J Cancer Res 2021;11(1):251-263
www.ajcr.us /ISSN:2156-6976/ajcr0119254

Original Article

The N and C-termini of SPCA2 regulate differently Kv10.1 function: role in the collagen 1-induced breast cancer cell survival

Alban Girault[1], Marta Peretti[1], Mehdi Badaoui[1,2], Anaïs Hémon[1], Hamid Morjani[3], Halima Ouadid-Ahidouch[1]

[1]Laboratory of Cellular and Molecular Physiology, UR UPJV 4667, University of Picardie Jules Verne, Amiens, France; [2]Department of Cell Physiology & Metabolism, University of Geneva, Faculty of Medicine, Geneva, Switzerland; [3]BioSpecT, EA7506, Faculty of Pharmacy, Reims University, Reims, France

Received July 30, 2020; Accepted September 1, 2020; Epub January 1, 2021; Published January 15, 2021

Abstract: It's now clearly established that the tumor microenvironment participates to tumor development. Among the different actors contributing to these processes, ion channels, located at the cancer cell surface, play a major role. We recently demonstrated that the association of Kv10.1, Orai1 and SPCA2 is crucial to promote the collagen-induced survival of MCF-7 breast cancer cells. By using siRNA directed against SPCA2, we shown that this protein is involved in the regulation of the activity, the expression and the sub-cellular localization of Kv10.1. In addition, it has been demonstrated that SPCA2 is involved in SICE in MCF-7 cells and that the N- and the C-terminal parts of this protein are necessary to interact and to produce Ca^{2+} entry. However, no information is available about the necessary SPCA2's important region to regulate Kv10.1. The aim of our work is to evaluate how SPCA2 could interact with Kv10.1 channel to induce survival promotion. By using different SPCA2 mutants, we evaluate the role of the N- and C-terminal sections on the expression and the activity of Kv10.1 channels. In addition, we analyzed the impact of these deletions on the collagen 1-induced cell survival. Our results bring out new information about the regulation of Kv10.1 channel through SPCA2. More specifically how the N- and C-terminus of this Ca^{2+} transporter regulate Kv10.1 expression, trafficking, and function suggesting new opportunities to target Kv10.1 channels in cancer progression.

Keywords: Kv10.1, SPCA2, orai1, breast cancer cells, tumor microenvironment

Introduction

Involvement of ion channels is now clearly established in tumor progression by using *in vitro* and preclinical mouse models. Since two decades, their roles in the cell proliferation, migration/invasion or therapy resistance have been well documented [1, 2]. In addition, more and more studies demonstrated that ion channels could act in cancer development in the form of complex. For instance, works from our laboratory demonstrated that BKCa channel interacts with the $IP3R_3$ or that TRPC1 could provide the Ca^{2+} entry mediated by the KCa3.1 channel to promote breast cancer cell proliferation [3, 4]. Association of Kv10.1 and Orai1 has also been highlight in breast cancer cells. In the high invasive model of MDA-MB-231 cells, this association regulates migration ability of the cells [5] while this ion channels complex regulates the survival of the less aggressive MCF-7 model [6]. Based on this accumulation of data, pharmacology of ion channels could thus offer new therapeutic options to cancer patients. However, a better comprehension of the underlying mechanisms is necessary to specifically target and modulate their function in cancer development in order to obtain the best benefits in combination with the actual therapeutic tools.

In addition to the ion channels, other transporters undergo expression or activity modifications over tumor progression. SPCA2, Secretory Pathway Ca^{2+}-ATPase type 2, has initially been described in the brain and involved in the lactation process in normal breast cells [7, 8]. More recently, this Ca^{2+} pump, especially localized in

the trans-golgi network, has been shown to participate to a Store-Independent Ca^{2+} Entry (SICE) through Orai1 channel in breast cancer cells that promote tumor progression [9]. Authors also demonstrated that N- and C-termini of SPCA2 cooperate to induce this Ca^{2+} influx. More precisely, the N-terminus is important to the binding to Orai1 while the C-terminus is necessary to the activation of Orai1. In addition, we recently demonstrated that SPCA2 participate to breast cancer cell survival in serum starvation condition [10].

Numerous information about the involvement of the tumor microenvironment (TME) are emerging. Indeed, modifications of the elements surrounding the tumor cells (stromal cells, immune cells, pH, hypoxia, extracellular matrix...) could participate to proliferation and aggressiveness regulation or to therapy resistance [11]. For example, it has been previously shown that collagen 1 expression is increased in more aggressive breast cancer phenotype [12]. We recently demonstrated that Kv10.1 potassium channel could interact with Orai1 calcium channel to promote survival properties of MCF-7 in presence of collagen 1 through a signaling pathway involving DDR-1 [6]. In addition, it has been demonstrated that Kv10.1 channels could interact with different proteins like epsin, 14-3-30 protein, PIST, which are able to modulate the expression and the activity of Kv10.1 channels in the brain [13]. Another work from our team deepened the role of this ion channels complex in the breast cancer cell survival process [10]. We demonstrated that Kv10.1 cooperates with Orai1 and SPCA2 promoting the survival capacity of MCF-7 cells in serum-starved condition and in presence of collagen 1. After the analysis of the Kv10.1, Orai1 and SPCA2 overexpression in 29 samples of breast cancer, we demonstrated that the 3 partners, by regulating SICE, are included in an auto-sustaining loop promoting the membrane expression of Kv10.1 and Orai1 that results in the survival stimulation. In addition, we showed that SPCA2 is co-immunoprecipitated with Kv10.1 and Orai1 and this Ca^{2+}-pump is co-localized with these two ion channels.

At the best of our knowledge, there is no information about the precise mechanism of Kv10.1's regulation through SPCA2. Based on the previously enounced data, we hypothesize that some SPCA2 regions could interact with Kv10.1, as it was demonstrated for Orai1. Thus, the aim of the present study is to decipher more precisely how SPCA2 could interact with Kv10.1 channel and consequently inducing survival promotion. By using SPCA2 mutants, presenting cleaved N- or C-extremities, we analyzed the impact of these constructions on expression, activities, localization and physiological effects. Our study is the first to look at the interactions between Kv10.1 and SPCA2 in order to open new avenues of research to develop innovative therapeutic tools to fight against the progression of breast cancer depending of Kv10.1.

Methods

Cell culture

MCF-7 cells (HTB-22; ATCC-LGC, Molsheim, France) were cultured in Eagle's Minimum Essential Medium (EMEM, Life Technologies, Saint-Aubin, France) supplemented with 5% fetal bovine serum (FBS, Life Technologies), 2 mM Glutamax and 0.06% HEPES (Life Technologies). Cells were maintained at 37°C in a humidified 5% CO_2-cotaining atmosphere. Absence of mycoplasma was routinely checked by using MycoAlert™ Mycoplasma Detection Kit (Lonza, Colmar, France). All experiments were conducted in the presence of collagen 1 coating (2.5 $\mu g/cm^2$) prepared has previously described [10]. The different assays were carried out according to the following sequence: transfected cells were seeded in complete medium supplemented with 5% FBS and the starvation was induced 24 h later by replacing it with a serum-free medium; analysis were finally conducted 48 h after the starvation.

Plasmid transfection

Transfection of cells was performed using nucleofection technology (Amaxa Biosystems, Lonza) according to the protocol previously described [10]. Cells were transiently transfected with plasmids encoding the different SPCA2 forms (Wild Type and N57, N101 and C927 mutants), a generous gift from the Professor Vangheluwe's group (Leuven), and used 72 h after transfection. For some experiments, cells were transfected simultaneously with siRNA directed against Kv10.1 (Dharmacon Research, Chicago, IL) or against Orai1 (Dharmacon Research).

qRT-PCR

Real Time PCR were conducted according to the protocol previously described [6]. Briefly, total RNA were extracted by using the standard Trizol-Phenol-Chloroform protocol and then quantified with a spectrophotometer (Nanodrop 2000, Wilmington, USA). cDNA was synthesized from 1 µg of total RNA with MultiScribeÔ Reverse Transcriptase (Applied Biosystems Carlsbad, USA). Primers used to the real time PCR presented the following sequences: Kv10.1 (forward 5'-CGCATGAACTACCTGAAGAC-3' and reverse 5'-TCTGTGGATGGGGCGATGTTC-3'), Orai1 (forward 5'-AGGTGATCAGCCTCAACGAC-3' and reverse 5'-CGTATCATGAGCGCAAACAG-3') and β-actin (forward 5'-CAGAGCAAGAGAGGCATCCT-3' and reverse 5'-ACGTACATGGCTGGGGTG-3'). Experiments were conducted on a LightCycler System (Roche, Basel, Switzerland) using a mix containing SYBRgreen.

Western blotting

Proteins were extracted, quantified and separated as previously described [6]. The primary antibodies used were: anti-Kv10.1 (1:200, Santa Cruz Biotechnology, Inc., Heidelberg, Germany), anti-Orai1 (1:200, Sigma Aldrich, Saint-Quentin-Fallavier, France), anti-SPCA2 (1:250, Santa Cruz Biotechnology, Inc.), anti-PARP (1:1500, Santa Cruz Biotechnology). GAPDH (1:3,000, Cell Signaling Tech.) antibody was used for loading control experiments. Detection and quantification were realized as previously described [6].

Biotinylation assays

To evaluate the distribution of Kv10.1 channels at the membrane level, biotinylation assays were conducted according to the following protocol. $8*10^5$ transfected cells were seeded in 60 mm petri dishes. After washing with cold PBS, cells were incubated with 2 mg of Sulfo-NHS-SS-biotin (Thermo Fisher Scientific, Rockford, IL) for 45-60 minutes at 4° with slight shaking. Addition of cold PBS containing 10 mM glycine allows the blocking of the reaction. Cells are then scraped in RIPA buffer. Almost 10 percent of the extract are stored to analyze the total protein fraction and the rest is incubated overnight at 4° with streptavidine agarose beads (Thermo Fisher Scientific) pre-washed with RIPA. After incubation, beads are washed 4-6 times with RIPA buffer. Proteins are eluted with 50 µl of Laemmli 2× and heating 60° for 30'. Denaturing SDS-PAGE has been used to separate proteins, which are then transferred onto nitrocellulose membranes and incubated with specifics antibodies for western blot.

Patch clamp experiments

The electrophysiological analysis was conducted has previously described [6]. Solutions used for the K^+ current recordings presented the following compositions (in mM): external: NaCl 140, KCl 5, $CaCl_2$ 2, $MgCl_2$ 2, glucose 5 and HEPES 10 at pH 7.4 (NaOH); internal: KCl 150, $MgCl_2$ 2, HEPES 10, EGTA 0.1, at pH 7.2 (KOH). For the store-independent calcium currents, the composition was (in mM): external: Na-gluconate 142, CsCl 10, $MgSO_4$ 1.2, $CaCl_2$ 2, glucose 10 and HEPES 10 at pH 7.4 (NaOH); internal: Cs-methanesulfonate 115, EGTA 10, $CaCl_2$ 5 (pCa 3.5), $MgCl_2$ 8, HEPES 10, at pH 7.2 (CsOH).

Immunofluorescence

Cells were fixed and permeabilized with iced-methanol for 20-30 minutes and blocked for 45-60 min with BSA 5%. The cells are then incubated for 90 min at room temperature in presence of the primary antibodies (Kv10.1, 1/200, Alomone Labs, Jerusalem, Israel; TGN-46 1/150, Invitrogen, Cergy-Pontoise, France). Cells are washed three times with PBS and incubated for 60 min with secondary antibodies conjugated to fluorophore (Alexa 550 for Kv10.1 staining 1/500, Invitrogen; Alexa 488 for TGN46 staining 1/500, ThermoFisher Scientific). After wash, cells were blocked again with BSA 5% for 45-60 min. Cells were then incubated overnight at 4°C with the second primary antibody. On the following day, cells were washed, incubated with the corresponding secondary antibody and counterstained with DAPI to visualize the nuclei. Fluorescence acquisitions were performed by using Axio Observer Z1 (Carl Zeiss MicroImaging, LLC, Oberkochen, Germany) and analyze with Fiji [14].

Statistical analysis

Data are presented as mean ± SEM (standard error of mean), n refers to the number of cells

or replicates, and N refers to the number of cell line passages. All the experiments were performed in at least 3 different cell lines passage number. Mean values of more than two groups were tested using one-way analysis of variance (ANOVA) followed by adequate *post hoc* tests, using GraphPad Prism version 5 (GraphPad Software, La Jolla, California, USA). Differences between the values were considered significant when $P<0.05$.

Results

SPCA2 mutants affect Kv10.1 expression

First, we evaluated the impact of the expression of two SPCA2 mutants presenting cleaved N-terminal extremity named N57 and N101, with the 57 or 101 first amino-acids cleaved, respectively, and one owning short C-terminal section (named C927), which does not possess the last 19 amino-acids, on the expression of both Kv10.1 and Orai1 (Figure S1). The different constructs are conjugated to mCherry. Transfections have been routinely checked by using western blot (Figure S1) and by fluorescence (data not shown).

Regarding Orai1 expression at the transcription or the translation level, no effect has been observed regardless of the transfected vector (Orai1 mRNA expression levels: N101: 0.98 ± 0.09; N57: 1.06 ± 0.15; C927: 0.89 ± 0.07; Orai1 protein expression levels: N101: 1.04 ± 0.09; N57: 0.82 ± 0.09; C927: 0.79 ± 0.28, **Figure 1B**, **1D** and **1F**). However, the analysis of the Kv10.1 expression presents major differences compared to Orai1. Kv10.1 mRNA is significantly reduced by 25% in the N57 transfected cells ($P<0.05$) and by 40% in the C927 transfected cells ($P<0.001$; **Figure 1A**). N101 transfection has no impact on the Kv10.1 mRNA level (0.88 ± 0.12). In addition, these observations were confirmed at the protein level (**Figure 1C** and **1E**). Indeed, we noted no effect of the N101 construction on the Kv10.1 total expression but a significant decrease with the N57 plasmid (almost 50% decrease, $P<0.05$) and a major reduction by 80% with the C927 construct ($P<0.001$, **Figure 1C** and **1E**).

All together, these results showed that only N57 and C927 constructs affect the mRNA and the protein expression of the Kv10.1 channel in the MCF-7 cells.

SPCA2 mutants alter potassium current through Kv10.1 channel and modify its cellular localization

Due to the alteration of the expression of the Kv10.1 mRNA and protein with the use of SPCA2 mutants, we then evaluated the impact of the construct transfections on the activity of the channels. Previously, we demonstrated that in our experimental condition, the largest contribution of the potassium conductance recorded in MCF-7 cells is due to Kv10.1 channel activity [6].

In MCF-7 cells transfected with the Wild type SPCA2 construct, the mean current density amplitude recorded at +60 mV is around 47.4 ± 10.5 pA/pF (**Figure 2A**). In the mutant transfected cells we observed a significant drastic decrease of the amplitude to 18.7 ± 1.5 ($P<0.05$), 18.9 ± 4.1 ($P<0.05$) and 12.4 ± 5.0 ($P<0.01$) pA/pF for the N101, N57 and C927 conditions respectively (**Figure 2A**, right panel).

In addition to the expression alteration, a modification of channel localization could be also responsible for the decreased Kv10.1 activity. We previously noted that silencing of SPCA2 could reduce the membrane enrichment of Kv10.1 in presence of collagen and starved condition [10]. We also observed that this channel has been stack in the Golgi apparatus when we used siRNA directed against SPCA2. We thus analyze the impact of the SPCA2 extremities' cleavages on the Kv10.1 localization by using immunofluorescence assays. Knowing that SPCA2 is localized in the trans Golgi network, the Golgi apparatus has been stained with anti-TGN-46 antibody [10]. In **Figure 2B**, we present staining for TGN-46 (green), Kv10.1 (red) and counterstaining of nuclei using DAPI (blue). In the WT condition, we observed that Kv10.1 channel is diffusedly marked throughout the cell with some membrane reinforcements and few yellow colorized points corresponding to co-localization of Kv10.1 and Golgi apparatus in the presence of collagen 1 as previously described [10]. However, in the presence of the different mutants (N57, N101 and C927), cells show increased similarity between the staining of Kv10.1 and of Golgi apparatus and the diffuse signal of the Kv10.1 staining is almost absent of the cells compared to the WT condition. We thus decided to conduct a com-

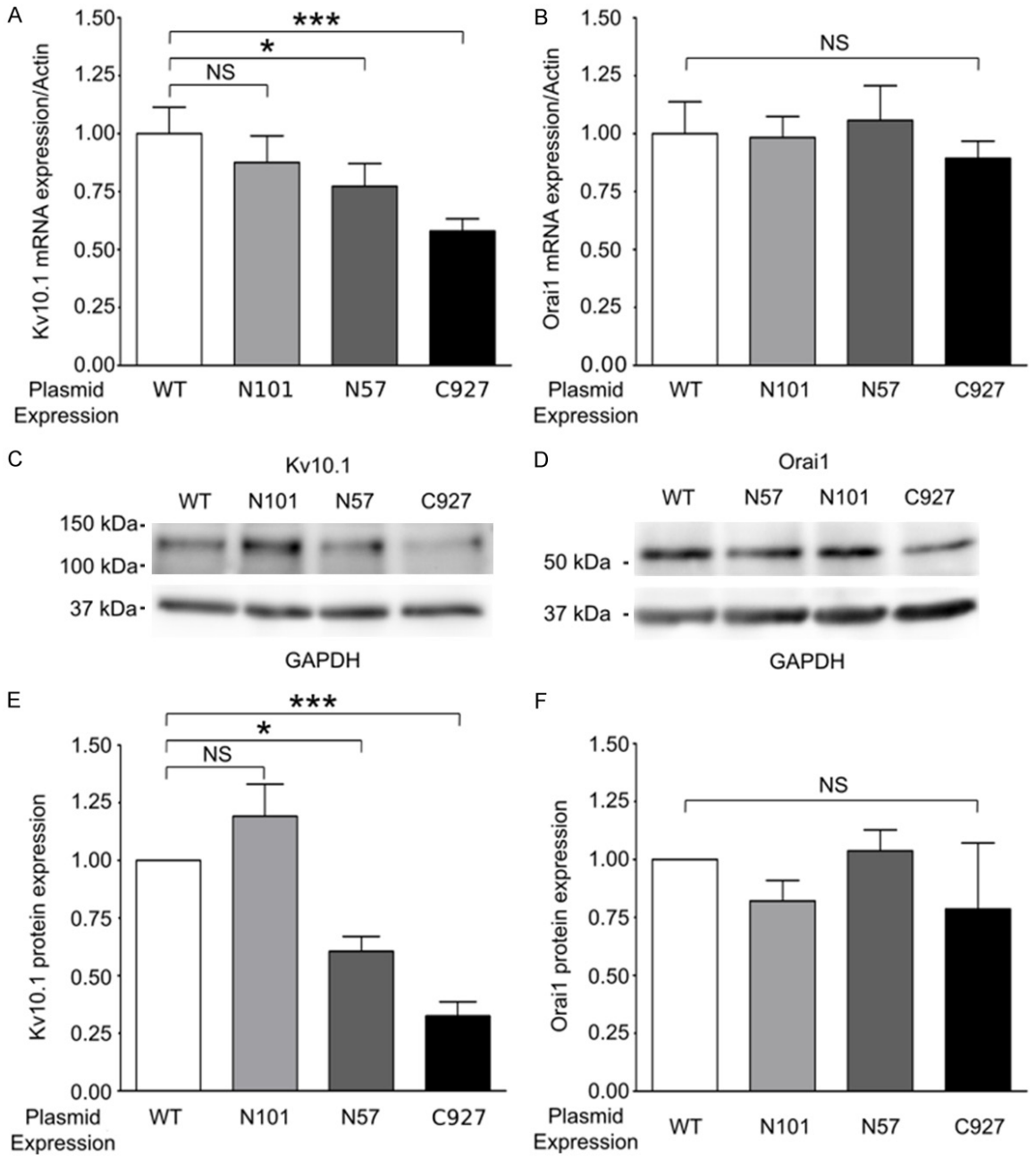

Figure 1. SPCA2's extremities are important in the regulation of Kv10.1 expression without affecting Orai1. Histograms representing the mRNA expression of Kv10.1 (A) and Orai1 (B) normalized to actin obtained by qPCR. mRNA have been extracted from MCF-7 cells, seeded on collagen 1, starved for 48 h, and transfected with plasmid containing the indicated vector (WT, N101, N57 and C927). Results are the average ± S.E.M of N=4, *P<0.05, ***P<0.001 (Anova followed by Dunnett's Multiple Comparison to the control Test). Representative western blots of Kv10.1 (C) and Orai1 (D) proteins levels in the similar conditions evaluated previously. Histograms present the densitometry analysis of the Kv10.1 (E) and Orai1 (F) protein expression. Results correspond to the average ± S.E.M of density analysis from N=5, *P<0.05, ***P<0.001 (Anova followed by Dunnett's Multiple Comparison to the control Test).

plementary analysis of the presence of the Kv10.1 channel at the membrane level by using biotinylation assays. This approach confirmed that Kv10.1 is less present at the membrane fraction when cells express the different mutants (Western blot representing from N=4; **Figure 2C**). It is interesting to note that N57 and C927 expressing cells showed an almost total absence of the channels at the membrane in correlation with the functional and the immu-

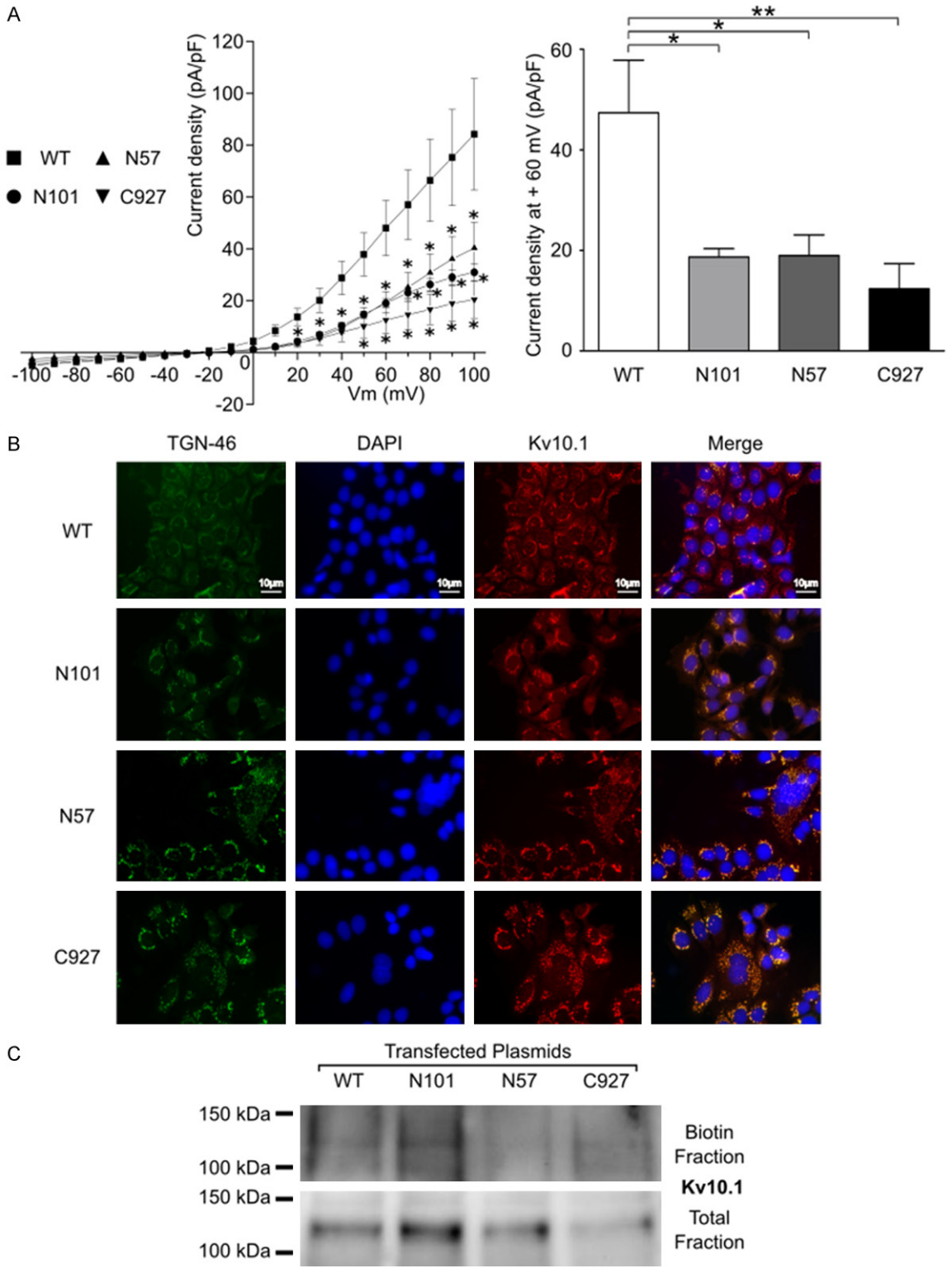

Figure 2. SPCA2 mutants affect Kv10.1 activity and cell localization. Kv10.1 activity recorded using whole cell configuration in WT-, N101-, N57- and C927-MCF-7 transfected cells seeded on collagen 1 and starved for 48 h. A. Graph present the current recorded after the application of a ramp protocol (500 msec from -100 to +100 mV, from a holding potential of -40 mV, left panel) and histograms represent the average ± SEM current densities at +60 mV (n=5-6 cells/condition), *P<0.05, **P<0.01 (Anova followed by Dunnett's Multiple Comparison to the control Test). B. Epifluorescence microscopy acquisition of MCF-7 cells stained with anti-TGN-46 (specific Golgi apparatus

marker) and anti-Kv10.1 antibodies in the different tested conditions. Yellow coloring in the merge column indicates the stacking of the Kv10.1 channels in the Golgi apparatus. Scale bar represents 10 µm. C. Representative western blot of 4 experiments showing the membrane fraction of Kv10.1 after biotinylation assay.

nostaining assays previously described. Our data suggest that the different SPCA2 mutants regulate Kv10.1 channel activity by regulating its expression and its plasma membrane trafficking.

Cooperation of Kv10.1 and SPCA2 to regulate calcium entry

It is well established that SPCA2 interacts with Orai1 and participates to the regulation of the Ca^{2+} signal in MCF-7 cells [9, 10]. In addition, we previously demonstrated that Kv10.1 also regulates the calcium entry through Orai1 in MCF-7 cells [15, 16]. We thus investigated the impact of the different SPCA2 constructs on the basal Ca^{2+} current and the contribution of Orai1 or Kv10.1. By using patch clamp, we observed a slight inhibition trend when the cells were transfected with N101 and C927 cleaved forms but not for the N57 mutant (**Figure 3A** and **3B**). In these conditions, the average Ca^{2+}-current density values at -120 mV are: WT: -3.2 ± 0.3 pA/pF, N101: -2.6 ± 0.2 pA/pF, N57: -3.9 ± 0.2 pA/pF and C927: -3.0 ± 0.4 pA/pF (**Figure 3B**).

In order to complete the analysis of the calcium current, we used the Mn^{2+} quench approach. Illustrative traces of the results obtained in tested conditions are presented in panels C and E of the **Figure 3**. In the N57 and N101 expressing cells, we observed no variations of the Ca^{2+} influx compared to the WT condition (WT: -0.82 ± 0.05 A.U.; N101: -79 ± 0.10 A.U.; N57: -0.82 ± 0.09 A.U.; **Figure 3C** and **3D**). However, in accordance with the literature that indicated the necessity of the SPCA2 C-term extremity to activate Orai1, we observed a significant decrease of the Ca^{2+} influx from -0.82 ± 0.05 A.U. to -0.49 ± 0.04 A.U, in the WT and C927 conditions respectively (**Figure 3D**, Anova P=0.016, WT *vs* C927 P<0.05).

In order to deepen the relationship of SPCA2's C-terminal extremity and the relation with the calcium signal, we transfected MCF-7 with specific Kv10.1 and Orai1 siRNAs to analyze impact of these co-transfection. As expected, siKv10.1 and siOrai1 induced drastic reduction of the calcium entry compared to the WT condition (respectively -0.39 ± 0.02 and -0.34 ± 0.04 A.U; **Figure 3E** and **3F**, Anova P=0.001, WT *vs* siKv10.1 P<0.001, WT *vs* siOrai1 P<0.001). C927 mutant expression induced similar reduction (-0.37 ± 0.09; WT *vs* C927 P<0.001). Interestingly, no additive effects have been observed in the co-transfected cells compared to the siRNA alone (C927 + siKv10.1: -0.29 ± 0.10; C927 + siOrai1: -0.29 ± 0.04). These results suggest a closed cooperation of the 3 partners in the regulation of Ca^{2+} homeostasis in MCF-7 cells, which is based more on the C-terminal extremity of SPCA2.

SPCA2 mutants affect the TME-induced MCF-7 survival

Finally, we evaluate the impact of the mutants' transfection on the TME-induced survival involving the trio Kv10.1-Orai1-SPCA2. Using flow cytometry, we evaluated the apoptosis rate after starvation in presence of collagen. We previously demonstrated that collagen promote cell survival after starvation. In addition, silencing of SPCA2 induce an increase in apoptosis rate [10]. Here, we observed that cells transfected with WT form present approximately 10% of apoptosis (**Figure 4A** and **4B**). No significant effect is observed in the N101 transfected cells. However, the N57 and C927 cells present significant increases of apoptosis to 20 and 25% respectively (**Figure 4B**, WT *vs* N57 P< 0.05, WT *vs* C927 P<0.01). A confirmation of this result has been obtained through the western blot analysis of PARP, a well-known protein involved in the programmed cell death [17]. We measured the evolution of the PARP status (full-length *vs* cleaved), in the different conditions. As shown in **Figure 4C** and **4D**, we observed that N101 failed to affect the expression of both the total PARP and cleaved proportion. At the opposite, N57 and C927 transfected cells present a significant reduction of the complete fraction (Anova P=0.0002, WT *vs* N57 P<0.01, WT *vs* C927 P<0.001, **Figure 4D**) associated to an increase of the cleaved proportion of PARP. In our experimental conditions, we observed major variations of the cleaved-PARP form inducing the lack of significance.

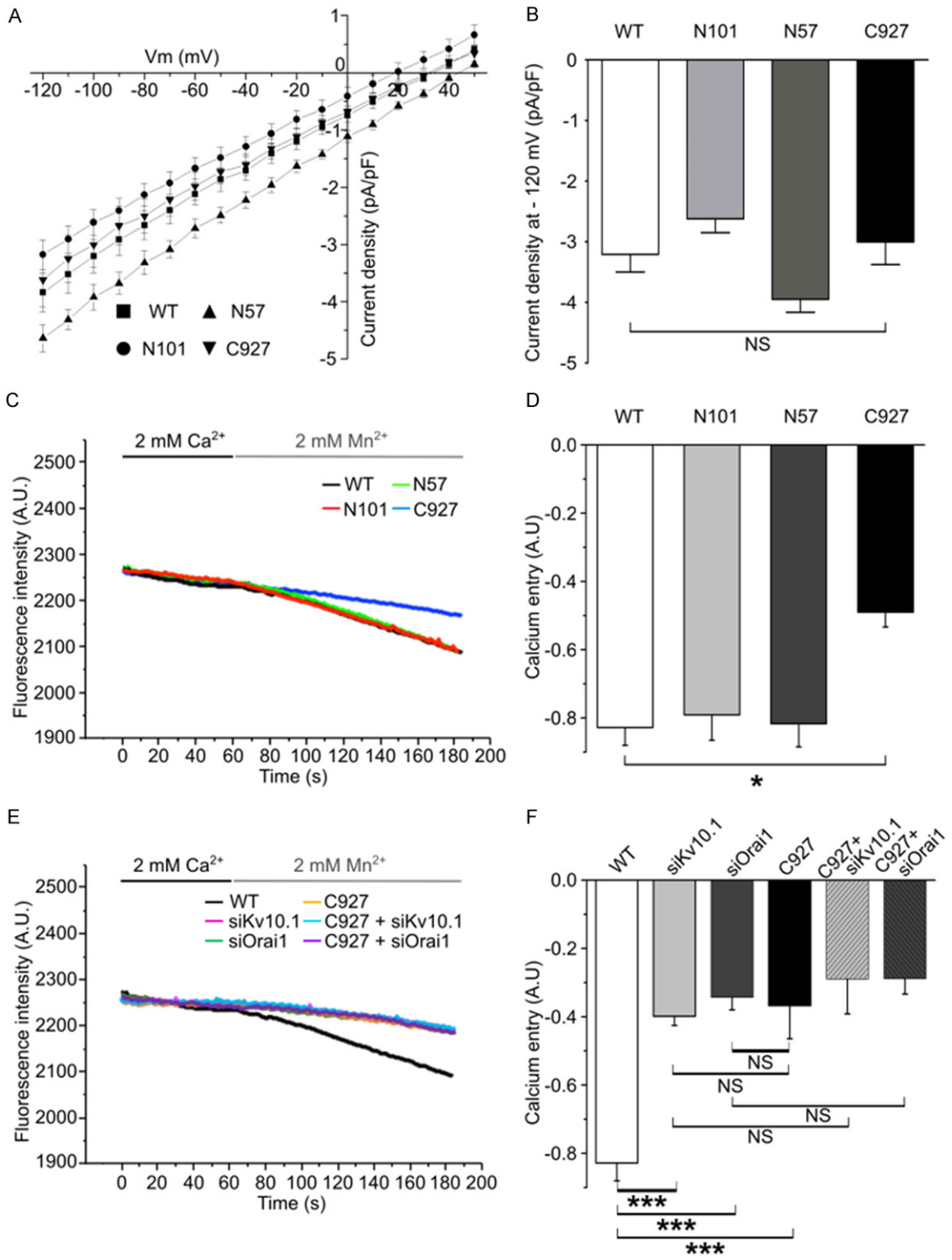

Figure 3. SPCA2's C-terminal extremity is involved in the Ca^{2+} entry. A. Basal calcium currents' patch clamp recordings. Whole cell currents recorded with specific bath solutions to record basal calcium currents in MCF-7 cells transfected with the different SPCA2 constructs. Cells were exposed to a 250 msec ramp protocol from -120 mV to +50 mV from a holding potential of -40 mV (left panel). B. The average current densities (± SEM) at -120 mV are presented by the histogram (right panel; n=6-10 cells/condition). C. Representative traces of Manganese quench imaging of cells transfected with the different mutants of SPCA2. D. Histograms representing the quantification of the basal calcium entry using Manganese quench imaging in MCF-7. (WT: n=140 cells, N101: n=96; N57: n=113; C927:

n=106; n=3). *P<0.05 (Anova followed by Dunnett's Multiple Comparison to the control Test). E. Representative traces of Manganese quench imaging of cells co-transfected with the C927 construct and siRNA directed against Kv10.1 and Orai1. F. Histograms representing the quantification of the basal calcium entry using Manganese quench imaging in MCF-7 cells transfected with C927 mutant in addition to siKv10.1 or siOrai1. (WT: n=140 cells, siKv10.1: n=115; siOrai1: n=61; C927: n=95; C927 + siKv10.1: n=84, C927 + siOrai1: n=72, n=3). ***P<0.001 (Anova followed by Dunnett's Multiple Comparison to the control Test).

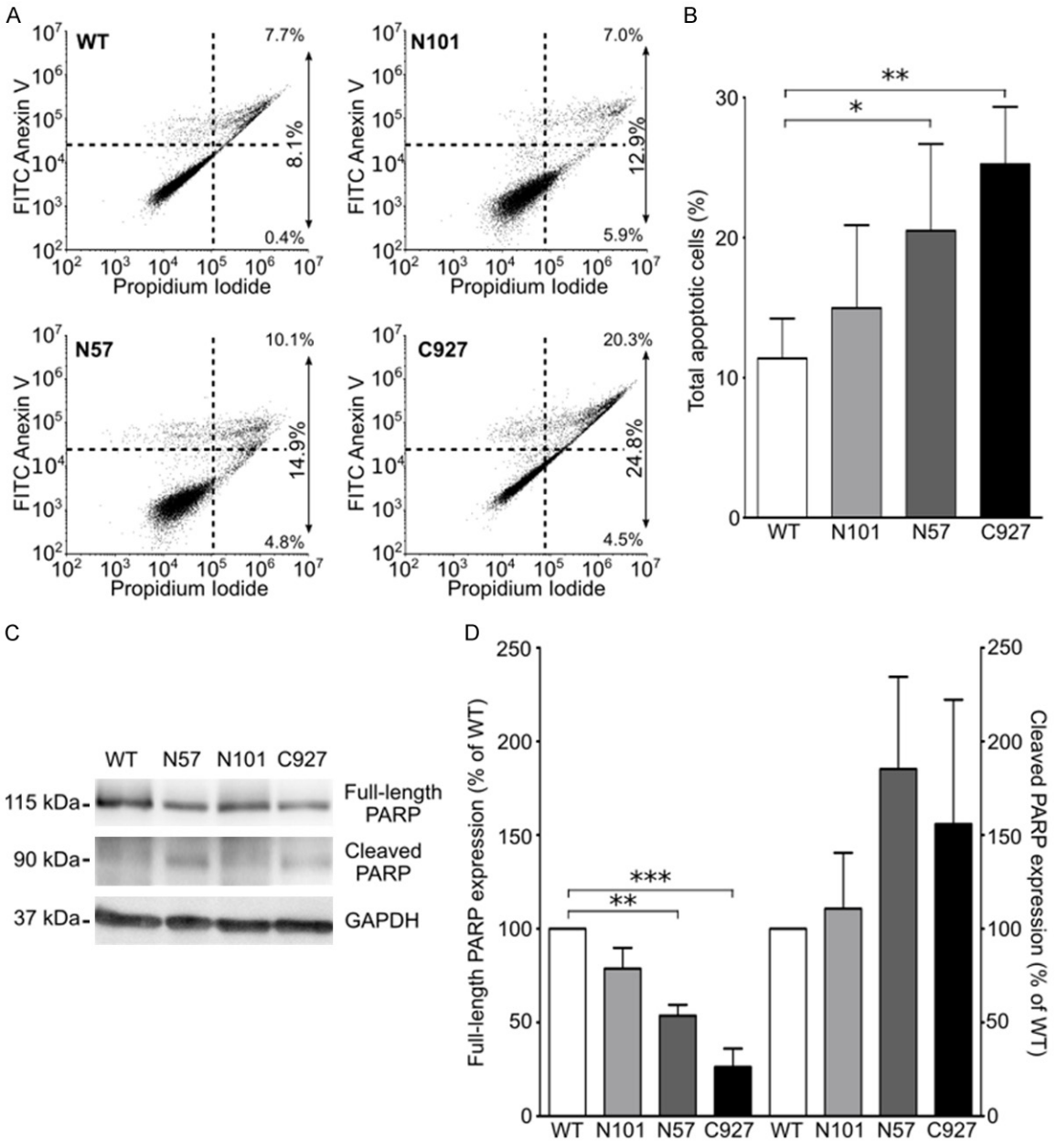

Figure 4. SPCA2 mutants interfere with the collagen 1-induced survival of MCF-7. After 48 h starvation, cell apoptosis assays are carried out by using annexin V/PI staining. A. Representative dot blots from one experiment. B. Histogram showing the mean proportion (± SEM) of apoptotic cells (n=4). *P<0.05, **P<0.01 (Anova followed by Dunnett's Multiple Comparison to the control Test). C. Representative western blot of full-length PARP and cleaved PARP protein levels in MCF-7 seeded on collagen after transfection with SPCA2 constructs and starvation for 48 h. D. Histograms representing the mean values ± SEM of the full-length or cleaved PARP expression levels normalized to GAPDH and compared to the WT condition. **P<0.01, ***P<0.001 (Anova followed by Dunnett's Multiple Comparison to the control Test).

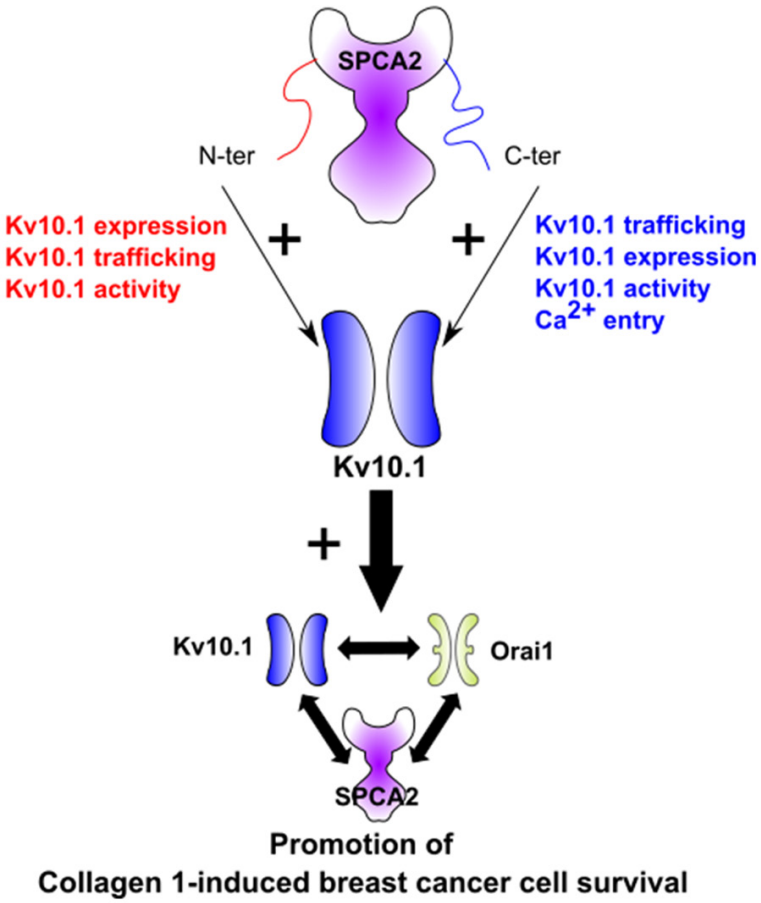

Figure 5. Schematic involvement of SPCA2 extremities in the regulation of Kv10.1, consequences on the collagen 1-induced MCF-7 cell survival. N-terminal extremity regulates Kv10.1 expression, function and subcellular localization. C-terminus is also involved in the control of the Kv10.1 expression, function and cell location and this extremity is additionally implicated in the regulation of Ca^{2+} entry. Kv10.1-Orai1-SPCA2 association is a major regulating complex of the collagen 1-induced MCF-7 survival after starvation.

In correlation to the expression and the function previously assayed, we demonstrated here that the SPCA2 N- and C-termini are important in the collagen-induced survival of MCF-7 cells.

Discussion

Ion channels are now classically described in the cancer cell biology to participate to tumor progression. Otherwise, breast cancer stays a major health issue requiring new way of medical management [18]. We recently demonstrated the role of the trio composed of Kv10.1, Orai1 and SPCA2 in the collagen 1-induced survival to starvation of breast cancer cells [10]. In this context, SPCA2 regulates the localization and the activity of the Kv10.1 and Orai1 channels to promote cell survival. Currently, little information is available about their trafficking and their regulation linked to transporter interactions. SPCA2-Orai interaction and regulation have already been described in normal and cancerous breast cells [9, 19]. In the present work, we demonstrated, for the first time, the important sections of SPCA2 involved in the regulation of the Kv10.1 channel in the context of breast cancer cells. SPCA2 N- and C-termini are differentially crucial to the regulation of the expression, the plasma membrane localization and therefore the activity of Kv10.1 (**Figure 5**).

We demonstrated that the lack of the amino-terminus extremity of SPCA2 affect the expression of Kv10.1 (**Figure 1**). In addition, we observed a drastic Kv10.1 activity decrease coupled to a rise of apoptotic cell number (**Figures 2** and **4**). Based on immunofluorescence assay results, we observed that the expression of N-terminus truncated SPCA forms provokes a partial stacking of Kv10.1 in the Golgi network (**Figure 2**). Together, these results suggest that the N-terminus extremity of SPCA2 is important in the expression, and the translocation of the Kv10.1 to the plasma membrane. In accordance with the work from other groups, we did not observe major effect on the Ca^{2+} signal. This result is consistent with the fact that SICE through Orai1 is dependent on the C-terminus of SPCA2 [9]. Consequently, the cleavage of the N-terminus extremity impacts at least partially the role of the trio in the collagen 1-induced survival of MCF-7 cells. In addition, it has been shown by Fenech and collaborators that a pancreas-specific form of SPCA2 presents a related structure to the N101 and N57 constructs used in our study [20, 21]. This pancreas-specific form presents a cleavage of the amino extremity. In their model, SPCA2 is localized in the endoplasmic

reticulum and not as classically in the Golgi apparatus. This observation is consistent with our results demonstrating that Kv10.1 is not exported to the cell membrane in absence of the SPCA2 N-terminus in MCF-7 cells expressing the N57 and N101 constructs. We noted discrepancies about the observed effects with the N57 and the N101 constructs on Kv10.1 channel. The N57 mutant induced a significant alteration of the localization, a reduction of the expression leading to reduction of K^+ flux that counteracted the pro-survival effect of the trio. While, the N101 construct, we only observed a reduction of the K^+ current associated to an alteration of the cellular location of the Kv10.1. From these results, we can suggest that the N-terminal extremity of SPCA2 possesses different functional domains may regulating the export and/or the function (location between the 57 and the 101 amino acids) and/or the expression of Kv10.1 (located in the 57 first amino acids). Smaardjik and colleagues also suggested that the conformational state is important to control Orai1-dependent SICE through the modification of intramolecular interactions between SPCA2 and Orai1 [22]. A similar concept could be responsive to the observed differences between the N57 and the N101 expressing cells.

Based on the data issued from our work, C-terminus extremity appears to be an important regulator of the Kv10.1 channel function in MCF-7 cells. Indeed, MCF-7 cells expressing the C927 construct present: i) a reduced expression of the channel (**Figure 1**), ii) a major decreased of Kv10.1 activity (**Figure 2**) due to iii) a localization in the golgi apparatus (**Figure 2**) associated to a reduction of the calcium entry (**Figure 3**). Consequently to the alteration of Kv10.1 function, the collagen 1-induced survival is largely affected (**Figure 4**). Our results thus suggest two possibilities to explain the relationship between the C-terminus extremity of SPCA2 and Kv10.1. In the first hand, the C-ter extremity of SPCA2 could directly interact with Kv10.1 to promote its function at the cell membrane level similarly to the relation observed with Orai1. In the second hand, Ca^{2+} could be in charge of the modification of Kv10.1 expression, localization and therefore function. Indeed, we previously demonstrated that the trafficking of Kv10.1 channel is Ca^{2+}-dependent [10] and it has been determined that the C-terminus extremity of SPCA2 is crucial to regulate Ca^{2+} entry [9]. Results obtained in the **Figure 3** support this concept.

An overview of the results obtained through this work explains at least partially the complexity of the Kv10.1-SPCA2-Orai1 partnership in the MCF-7 cells. It is interesting to note that the results previously observed by using siRNA directed against SPCA2 conducting to the reduction of the survival capacity [10] correspond to the accumulation of an alteration of the expression and function of Kv10.1 (causing by the lack of C- or N-termini) and a modification of the trafficking (due to at least in part by the N-terminus section of SPCA2). Results presented here are focused about the regulation of Kv10.1, which is an important trigger of the complex in the breast cancer cell survival process. However, it should be interesting to evaluate the role of this potassium channel associated to Orai1 and SPCA2 and the underlying regulatory mechanism in other cancer cell functions like migration, invasion or epithelial-to-mesenchymal transition (EMT). Indeed, the different actors implied in the complex are already known to be implicated in these different phenomena. For example, it has been recently shown that SPCA2 promotes the epithelial status of breast cancer cell by regulating the E-cadherin biogenesis [23].

Conclusion

Current studies reported the important role of the microenvironment in the tumor progression by, for example, influencing therapeutic response [24] or hijacking normal cells to promote the development [25]. In addition, ion channels are now clearly involved in the tumor adaptation to microenvironment evolution [26-28]. Our work highlights a new mechanism for regulating Kv10.1 channel in breast cancer cells. Indeed, SPCA2, by regulating the expression, the trafficking and the function of Kv10.1, regulates the collagen 1-induced survival in MCF-7 cells. Our results show a putative new approach to target mechanism influencing the breast cancer response to microenvironment or to characterize the status of breast cancer cell.

Acknowledgements

MB was a recipient of founding from the Ministère de l'Enseignement Supérieur et de la Recherche. MP is recipient of founding from the

Conseil Régional de Picardie. This work was supported by the Région Hauts-de-France (Picardie) and the FEDER (Fonds Européen de Développement Economique Régional), the Université Picardie Jules Verne, the Ligue Contre le Cancer (Septentrion) and the SFR CAP-Santé (FED 4231). We want to acknowledge Dr L. Gutierrez and Dr S. Guénin to the access at the Centre de Ressources Régionales en Biologie Moléculaire (CRRBM) and to their scientific and technical advices.

Disclosure of conflict of interest

None.

Abbreviations

Ca^{2+}, calcium; SPCA2, Secretory Pathway Ca^{2+}-ATPase type 2; SICE, Store-Independent Ca^{2+} Entry; TME, Tumor MicroEnvironment; DDR1, Discoidin Domain Receptor 1.

Address correspondence to: Halima Ouadid-Ahidouch and Alban Girault, Laboratory of Cellular and Molecular Physiology, UR UPJV 4667, University of Picardie Jules Verne, Amiens, France. E-mail: hasciences@u-picardie.fr (HOA); alban.girault@u-picardie.fr (AG)

References

[1] Prevarskaya N, Skryma R and Shuba Y. Ion channels in cancer: are cancer hallmarks oncochannelopathies? Physiol Rev 2018; 98: 559-621.

[2] Kischel P, Girault A, Rodat-Despoix L, Chamlali M, Radoslavova S, Abou Daya H, Lefebvre T, Foulon A, Rybarczyk P, Hague F, Dhennin-Duthille I, Gautier M and Ouadid-Ahidouch H. Ion channels: new actors playing in chemotherapeutic resistance. Cancers (Basel) 2019; 11: 376.

[3] Faouzi M, Hague F, Geerts D, Ay AS, Potier-Cartereau M, Ahidouch A and Ouadid-Ahidouch H. Functional cooperation between KCa3.1 and TRPC1 channels in human breast cancer: role in cell proliferation and patient prognosis. Oncotarget 2016; 7: 36419-36435.

[4] Mound A, Rodat-Despoix L, Bougarn S, Ouadid-Ahidouch H and Matifat F. Molecular interaction and functional coupling between type 3 inositol 1,4,5-trisphosphate receptor and BKCa channel stimulate breast cancer cell proliferation. Eur J Cancer 2013; 49: 3738-3751.

[5] Hammadi M, Chopin V, Matifat F, Dhennin-Duthille I, Chasseraud M, Sevestre H and Ouadid-Ahidouch H. Human ether a-gogo K(+) channel 1 (hEag1) regulates MDA-MB-231 breast cancer cell migration through Orai1-dependent calcium entry. J Cell Physiol 2012; 227: 3837-3846.

[6] Badaoui M, Mimsy-Julienne C, Saby C, Van Gulick L, Peretti M, Jeannesson P, Morjani H and Ouadid-Ahidouch H. Collagen type 1 promotes survival of human breast cancer cells by overexpressing Kv10.1 potassium and Orai1 calcium channels through DDR1-dependent pathway. Oncotarget 2018; 9: 24653-24671.

[7] Faddy HM, Smart CE, Xu R, Lee GY, Kenny PA, Feng M, Rao R, Brown MA, Bissell MJ, Roberts-Thomson SJ and Monteith GR. Localization of plasma membrane and secretory calcium pumps in the mammary gland. Biochem Biophys Res Commun 2008; 369: 977-981.

[8] Xiang M, Mohamalawari D and Rao R. A novel isoform of the secretory pathway Ca2+, Mn(2+)-ATPase, hSPCA2, has unusual properties and is expressed in the brain. J Biol Chem 2005; 280: 11608-11614.

[9] Feng M, Grice DM, Faddy HM, Nguyen N, Leitch S, Wang Y, Muend S, Kenny PA, Sukumar S, Roberts-Thomson SJ, Monteith GR and Rao R. Store-independent activation of Orai1 by SPCA2 in mammary tumors. Cell 2010; 143: 84-98.

[10] Peretti M, Badaoui M, Girault A, Van Gulick L, Mabille MP, Tebbakha R, Sevestre H, Morjani H and Ouadid-Ahidouch H. Original association of ion transporters mediates the ECM-induced breast cancer cell survival: Kv10.1-Orai1-SPCA2 partnership. Sci Rep 2019; 9: 1175.

[11] Hui L and Chen Y. Tumor microenvironment: sanctuary of the devil. Cancer Lett 2015; 368: 7-13.

[12] Kauppila S, Stenback F, Risteli J, Jukkola A and Risteli L. Aberrant type I and type III collagen gene expression in human breast cancer in vivo. J Pathol 1998; 186: 262-268.

[13] Cazares-Ordonez V and Pardo LA. Kv10.1 potassium channel: from the brain to the tumors. Biochem Cell Biol 2017; 95: 531-536.

[14] Schindelin J, Arganda-Carreras I, Frise E, Kaynig V, Longair M, Pietzsch T, Preibisch S, Rueden C, Saalfeld S, Schmid B, Tinevez JY, White DJ, Hartenstein V, Eliceiri K, Tomancak P and Cardona A. Fiji: an open-source platform for biological-image analysis. Nat Methods 2012; 9: 676-682.

[15] Borowiec AS, Hague F, Gouilleux-Gruart V, Lassoued K and Ouadid-Ahidouch H. Regulation of IGF-1-dependent cyclin D1 and E expression by hEag1 channels in MCF-7 cells: the critical role of hEag1 channels in G1 phase progression. Biochim Biophys Acta 2011; 1813: 723-730.

[16] Ouadid-Ahidouch H and Ahidouch A. K+ channel expression in human breast cancer cells: involvement in cell cycle regulation and carcinogenesis. J Membr Biol 2008; 221: 1-6.
[17] Herceg Z and Wang ZQ. Functions of poly(ADP-ribose) polymerase (PARP) in DNA repair, genomic integrity and cell death. Mutat Res 2001; 477: 97-110.
[18] Ferlay J, Colombet M, Soerjomataram I, Mathers C, Parkin DM, Pineros M, Znaor A and Bray F. Estimating the global cancer incidence and mortality in 2018: GLOBOCAN sources and methods. Int J Cancer 2019; 144: 1941-1953.
[19] Cross BM, Hack A, Reinhardt TA and Rao R. SPCA2 regulates Orai1 trafficking and store independent Ca2+ entry in a model of lactation. PLoS One 2013; 8: e67348.
[20] Fenech MA, Carter MM, Stathopulos PB and Pin CL. The pancreas-specific form of secretory pathway calcium ATPase 2 regulates multiple pathways involved in calcium homeostasis. Biochim Biophys Acta Mol Cell Res 2020; 1867: 118567.
[21] Fenech MA, Sullivan CM, Ferreira LT, Mehmood R, MacDonald WA, Stathopulos PB and Pin CL. Atp2c2 is transcribed from a unique transcriptional start site in mouse pancreatic acinar cells. J Cell Physiol 2016; 231: 2768-2778.
[22] Smaardijk S, Chen J, Wuytack F and Vangheluwe P. SPCA2 couples Ca(2+) influx via Orai1 to Ca(2+) uptake into the Golgi/secretory pathway. Tissue Cell 2017; 49: 141-149.
[23] Dang DK, Makena MR, Llongueras JP, Prasad H, Ko M, Bandral M and Rao R. A Ca(2+)-ATPase regulates E-cadherin biogenesis and epithelial-mesenchymal transition in breast cancer cells. Mol Cancer Res 2019; 17: 1735-1747.
[24] Wu T and Dai Y. Tumor microenvironment and therapeutic response. Cancer Lett 2017; 387: 61-68.
[25] Arneth B. Tumor microenvironment. Medicina (Kaunas) 2019; 56: 15.
[26] Girault A, Ahidouch A and Ouadid-Ahidouch H. Roles for Ca(2+) and K(+) channels in cancer cells exposed to the hypoxic tumour microenvironment. Biochim Biophys Acta Mol Cell Res 2020; 1867: 118644.
[27] Mohr CJ, Steudel FA, Gross D, Ruth P, Lo WY, Hoppe R, Schroth W, Brauch H, Huber SM and Lukowski R. Cancer-associated intermediate conductance Ca(2+)-activated K(+) channel KCa3.1. Cancers (Basel) 2019; 11: 109.
[28] Petho Z, Najder K, Bulk E and Schwab A. Mechanosensitive ion channels push cancer progression. Cell Calcium 2019; 80: 79-90.

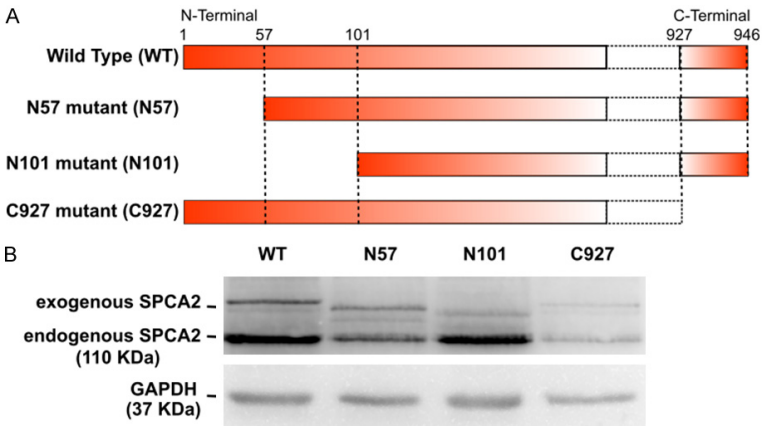

Figure S1. Schematic representation of constructs used in the study and transfection's validation by using western blot. A. SPCA2 wild type form has a complete sequence of 946 amino acids. Mutants present N-terminal or C-terminal extremities cleaved i.e. N57, the first 57 amino acids, N101, the first 101 amino acids, and C927, the last 19 amino acids. Every constructs are conjugated to M-cherry. Generous gift from the Professor Vangheluwe's group (Leuven). B. Representative western blot showing the endogenous and the exogenous expression of SPCA2. Exogenous SPCA2 constructs present higher molecular weight due to the presence of the conjugated M-cherry.